Master of Science

Human relevance of the statin-induced proliferative changes in the livers of rodents

The Graduate School

of the University of Ulsan

Department of Medical Science

Jang Mi Lee

Human relevance of the statin-induced proliferative changes in the livers of rodents

Supervisor: Woo-Chan Son

A Dissertation

Submitted to
the Graduate School of the University of Ulsan
In partial Fulfillment of the Requirements
for the Degree of

Master of Science

by

Jang Mi Lee

The Graduate School
of the University of Ulsan
Department of Medical Science
August 2022

Human relevance of the statin-induced proliferative changes in the livers of rodents

This certifies that the master's thesis

of Jang Mi Lee is approved.

_____

Committee Chair Dr. Kyun-Seop Bae

_____

Committee Member Dr. Jong Hoa Ok

_____

Committee Member Dr. Woo-Chan Son

Department of Medical Science

University of Ulsan, Korea

August 2022

ABSTRACT

In rodents, hepatic proliferative changes are the most common seen in toxicity studies. Hepatomegaly without histologic or clinical pathology alterations indicative of liver toxicity is considered an adaptive and a non-adverse reaction whereas hepatomegaly is also considered that its perceived relevance to hepatotoxicity, to carcinogenicity frequently in long term studies. However, human relevance of the findings are various dependent on the mechanisms of action, even if carcinogenicity observed in rodents, may be considered of no relevance to humans depending on the mechanisms.

Hepatomegaly, often observed in preclinical toxicity studies in rodents, may be indicated by hepatic microsomal cytochrome P450s (CYPs). Hepatic enzyme induction is series of metabolic reactions to xenobiotics associated with increases in liver weight, morphological changes in hepatocytes, and induction of *CYP* gene expression. Morphological features of hepatic enzyme induction range from adaptive physiological responses characterized by liver weight increases with or without hepatocellular hypertrophy to adverse pathological effects including toxicity and carcinogenicity. The morphological responses can be assessed by light and electron microscopy and immunohistochemistry and should be interpreted in conjunction with clinical pathology alterations to determine when an adaptive response becomes adverse.

Cytochrome P450s (CYPs) are important heme-containing proteins that play important roles in the metabolism of xenobiotics and endogenous compounds, and most CYP forms are induced by nuclear receptor-mediated mechanisms leading to an increase in CYP gene transcription. The main mechanisms by which metabolic enzymes are

derived include nuclear hormone receptors such as aryl hydrocarbon receptor (AhR), constitutional and rostane receptor (CAR), and pregnane X receptor (PXR). In the case of rodents, peroxisome predictor-activated receptor α (PPARα) is also involved. When the nuclear receptors CAR, PXR, or PPARα are activated, they are regarded as highly sensitive, rodent-specific responses and are not well correlated with responses in humans. These are known to increase gene transcription of drug-metabolizing enzymes such as CYP1A1, CYP2B10, CYP3A, and CYP4A, respectively. It is important to clarify the mechanisms of liver proliferative changes as the human relevance varies depending on which mechanisms cause the lesions, and the conclusion should be reached through an integrative weight of evidence approach.

This is a follow-up study to understand the mechanism of hepatic neoplasm development observed in a 24-month carcinogenicity study of the statin in ICR mice and to determine whether the changes were correlated with humans.

The statin-based test article was administered once per day via oral gavage at a low dose (500 mg/kg) and high dose (3200 mg/kg) for 56-days in ICR mice to mimic the previous study. In addition, positive controls TCDD, TCPOBOP, rifampicin, and DEHP were selected for comparative analysis of CYP expression and administered once daily via oral gavage at appropriate doses for the duration of drug administration. These compounds are known to activate the nuclear hormone receptors AhR, CAR, PXR, and PPARα, respectively. Afterward, parameters, including body and organ weights, serum biochemistry, histological examination of the liver, quantitative real-time PCR (RT-qPCR), and Immunohistochemistry were determined.

The results suggest that statin-based drug induced hepatic proliferative changes are caused by the induction of the CYP3A subfamily, which is mediated by PXR activation, and the histologic changes induced by the statin may be less relevant in humans.

Keywords : Cytochrome P450 (CYP); Enzyme induction; Hepato-carcinogenesis; Hepatocellular hypertrophy; Hepatomegaly; Nuclear hormone receptor

Contents

LIST OF FIGURES AND TABLES

ABBREVIATION

AhR, aryl hydrocarbon receptor

ALP, alkaline phosphatase

ALT, alanine aminotransferase

AST, aspartate aminotransferase

CAR, constitutional and rostane receptor

CC1/2, cell conditioning solutions

CYP, cytochrome P450

DEHP, di(2-ethylhexyl)phthalate

DMSO, dimethyl sulfoxide

EDTA, ethylenediaminetetraacetic acid

H&E, hematoxylin and eosin

IACUC, Institutional Animal Care and Use Committee

IHC, immunohistochemistry

PPAR, peroxisome proliferator-activated receptor

PXR, pregnane X receptor

RBCs, red blood cells

RT-qPCR, quantitative real-time PCR

SD, standard deviation

TCDD, 2,3,7,8-tetrachlorodibenzo-p-dioxin

TCPOBOP, 1,4-bis[2-(3,5-dichloropyridyloxy)]benzene

I. INTRODUCTION

Xenobiotics induce microsomal enzymes (cytochrome P450s, CYPs) responsible for their metabolism to promote their removal [1]. Chemical-induced hepatic proliferative changes, often observed in preclinical toxicity studies in rodents, are likely to lead to hepatomas. Hepatomegaly, which are non-histologic or -clinical pathology alterations indicative of liver toxicity, is considered an adaptive and non-adverse reaction. Hepatocellular hypertrophy after xenobiotic exposure is similar to the induction of cytochrome P450s (CYPs) and other drug-metabolizing enzymes [2]. These changes are commonly observed after drug administration in rodents [3].

CYPs are important heme-containing proteins that play important roles in the metabolism of xenobiotics and endogenous compounds [4]; most CYP isoforms are induced by nuclear- receptor-mediated mechanisms that lead to increased *CYP* gene transcription. Metabolic enzymes are mainly induced by the following mechanisms: nuclear hormone receptors, such as the aryl hydrocarbon receptor (AhR), constitutional and rostane receptor (CAR), and pregnane X receptor (PXR) [5]. In rodents, the peroxisome predictor-activated receptor α (PPARα) is also involved. Due to ligand activation of these receptors, transcription of the *CYP1A1, CYP2B10, CYP3A*, and *CYP4A* are increased, respectively. Nuclear receptor activation is a molecular initiating event of the pathway(s) leading to different adverse effects in the liver [6].

The aryl hydrocarbon receptor (AhR) induces multiple drug-metabolizing enzymes, such as CYP1A1, CYP1A2 and CYP2B1. 2,3,7,8-Tetrachlorodibenzo-p-dioxin (TCDD) is a potent activator of AhR and, causes liver enlargement due to hepatocyte hypertrophy, multinucleated hepatocytes, fatty changes, necrosis, and increased cellular replication

with suppression of apoptosis resulting in the eventual outgrowth of enzyme altered hepatic foci and hepatocarcinogenesis [7-11].

Constitutive androstane receptor (CAR) is activated by potent drug-metabolizing enzyme derivatives, such as phenobarbitone, and increased expression of *Cyp2b10* and several other genes in mice [12]. The pesticide contaminant 1,4-bis[2-(3,5-dichloropyridyloxy)]benzene, referred to as TCPOBOP, is considered to be the most potent of this group of inducers [13]. Activation of CAR is associated with substantial proliferation of smooth endoplasmic reticulum (SER), causing hepatocellular hypertrophy [14]. When proliferation of smooth endoplasmic reticulum occurs due to enzyme induction, eosinophilic ground-glass forms are observed in the cytoplasm.

The pregnane X receptor (PXR) is the main regulator of *CYP3A* gene transcription in rodent and is similarly involved in liver metabolism and is associated with liver metabolism [15]. For example, the antibiotic rifampicin, a front-line treatment for tuberculosis, is an established PXR agonist [15, 16].

Peroxisome proliferator-activated receptor alpha (PPARα) is specifically associated with peroxisome proliferation and hepatocellular hypertrophy in rodents [17, 18]. When PPARα is activated, it stimulates the proliferation of hepatocellular peroxisomes and induces CYP4A in mice and rats [19, 20]. Peroxisome proliferation is often accompanied by eosinophilic granules in the cytoplasm. Di(2-ethylhexyl)phthalate (DEHP), a widely used plasticizer, is a potential non-genotoxic carcinogen that transactivates PPARα [18].

When CAR, PXR, or PPARα are activated, they are regarded as highly sensitive rodent-specific responses and are not well correlated with responses in humans. However, the mode of action for AhR mediated carcinogenesis could not be excluded

for humans [21].

Hepatomegaly is perceived as an indicator of hepatotoxicity and frequently as an indicator of carcinogenicity in long-term studies [21, 22]. However, hepatomegaly without changes in histologic or clinical pathology indicative of liver toxicity is considered an adaptive and non-adverse reaction [21]. Therefore, it is important to understand the mechanisms of hepatocellular hypertrophy and hepatocarcinogenesis, and an integrative weight of evidence approach should be used. A weight of evidence assessment is a familiar concept found in scientific and regulatory literature, it is generally understood as a method for decision making that involves consideration of multiple sources of information and lines of evidence [23].

Therefore, a mechanistic study was conducted to determine whether hepatic proliferative changes observed in the carcinogenicity study of the statin in ICR mice could be correlated with changes in humans.

II. MATERIALS AND METHODS

1. Experimental design

ICR mice (approximately 6-weeks-old) purchased from Orient Bio (Gyeonggi-do, Korea) were used in these experiments. A total of 56 male and 56 female mice were randomized into 7 groups of 16 mice each (8 males and 8 females in each group). Mice were housed in a specific pathogen-free facility in a climate-controlled room with a temperature of 22±2℃, humidity of 55±5%, and a 12-hour dark-light cycle. This study was conducted in accordance with the regulations of the Institutional Animal Care and Use Committee of Asan Medical Center (Permit Number: 2021-02-150).

To mimic the previous study, the test article, HMG-CoA reductase inhibitor (the statin) in 0.25% methyl cellulose solution was administered once per day via oral gavage at low (500 mg/kg) and high doses (3200 mg/kg) for 56 days. The doses were established in a previous study. The control group was given 0.25% methyl cellulose instead of the statin. The positive control groups were administered TCDD, TCPOBOP, rifampicin, or DEHP once per day via oral gavage at appropriate doses. The dosages of the positive control groups were selected to be sufficient to induce hepatomegaly based on a literature reviews and preliminary studies. The positive control groups were considered for comparative analysis of CYP expression.

Body weights were measured 1 day after the last administration was performed. Details of the experimental groups are given in **Table 1**.

Table 1. Experimental design for *in vivo* study.

Group	Vehicle	Dose (mg/kg)	Volume (mL/kg)	Administrations (days)	No. of animals	
					Male	Female
CONTROL	0.25% MC	-	10	56	8	8
(Statin) LOW	0.25% MC	500	10	56	8	8
(Statin) HIGH	0.25% MC	3200	10	56	8	8
TCPOBOP	10% DMSO in corn oil	10	10	7	8	8
Rifampicin	DMSO	80	10	7	8	8
DEHP	DMSO	100	10	7	8	8
TCDD	10% acetone in corn oil	15 ug/kg	10	2	8	8

MC: methyl cellulose

DMSO: dimethyl sulfoxide

2. Serum biochemistry

All animals were anesthetized with Terrell isoflurane (Piramal Pharma Solutions, Sellersville, PA, USA), and blood was collected from the inferior vena cava after 12 hours of fasting; the animals were killed by exsanguination. Whole blood was collected in serum-separating tubes (BD Microtainer^{R}, 365967; Becton Dickinson, Franklin Lakes, NJ, USA) and mixed thoroughly. The blood was centrifuged at 3,000 rpm for 10 minutes to isolate the serum, which was used for clinical serum biochemistry analysis. In this study, alanine aminotransferase (ALT), aspartate aminotransferase (AST), alkaline phosphatase (ALP), total bilirubin (TBIL), triiodothyronine (T3), glucose, total protein (TP), and cholesterol levels were measured using an automated clinical chemistry analyzer (Hitachi, 7180 Clinical Analyzer; Hitachi Ltd., Tokyo, Japan).

3. **Histopathological evaluation**

The liver and thyroid glands were fixed in 10% neutral-buffered formalin (MDPOS, 50-00-0) for 24-48 hours. Then they were dehydrated in graded ethanol, cleared in xylene using a Shandon Excelsior ES tissue processor (Thermo Fisher Scientific, Walthan, MA, USA), and embedded in paraffin blocks using an EG1150H paraffin-embedding station (Leica Biosystems, Wetzlar, Germany). The paraffin blocks were sectioned to 3-μm thicknesses and mounted on slides (MUTO, 5116-20F). The sections were baked in a 65℃ dry oven for 30-60 minutes and stained with hematoxylin and eosin (ST5010 Autostainer XL Slide Stainer, Leica Biosystems).

4. Immunohistochemical assessment

For identifying the expression of the CYP450 (CYP1A, CYP2B, CYP3A, and CYP4A subfamilies) proteins, immunohistochemical staining of the liver sections was performed using an automated slide preparation system (Benchmark XT; Ventana Medical Systems Inc., Tucson, AZ, USA). Paraffin-embedded blocks of ICR mice liver tissue were cut into 3-μm thick slices, and the sections were mounted on coated glass slides (MUTO, 5116-20F-C). The sections were baked in a 65℃ dry oven for 30-60 minutes. Deparaffinization, antigen retrieval and immunostaining were performed according to the manufacturer's instructions with EZ Prep Concentration, Cell Conditioning Solutions (CC1, CC2) and the UltraView Universal DAB Detection Kit (Ventana Medical Systems, Inc.). Then the liver sections were stained with primary antibodies (**Table 2)** for 36 minutes at 37℃. UltraMap Anti-Ms/Rb HRP (Ventana Medical Systems Inc., Tucson, AZ) was used as a secondary antibody for 4 or 12 minutes (**Table 2**). Immuno-stained sections were counterstained with hematoxylin and bluing reagent, and a coverslip was mounted using lipid-soluble mounting medium.

Table 2. Information about antibodies used for immunohistochemical staining.

Antibody	Cat. No.	Manufacturer	Host	Type	Dilution	Incubation time ($1^{st}/2^{nd}$)
Anti-CYP1A1	ab79819	Abcam Inc.	Rabbit	Monoclonal	1:100	36m/12m
Anti-CYP2B10	sc-73546	Santa Cruz Biotechnology	Mouse	Monoclonal	1:1000	36m/4m
Anti-CYP3A4	ab197053	Abcam Inc.	Rabbit	Polyclonal	1:500	36m/12m
Anti-CYP4A	sc-271983	Abcam Inc.	Mouse	Polyclonal	1:1000	36m/4m

5. Quantitative real-time PCR

5.1. Primer design

The gene symbol and sequence for each candidate reference gene was retrieved with the assistance of the Primer3 program [24] available at https://bioinfo.ut.ee/primer3-0.4.0/. The primer sequences are provided in **Table 3**.

5.2. RNA purification/extractions and cDNA synthesis

At necropsy, a portion of the left lobe of the liver was collected separately and placed in a cryotube before the liver was fixed in 10% NBF. The cryotubes were immediately preserved in liquid nitrogen and were subsequently moved to a deep freezer and preserved at −80°C within 2 hours of collection until processing for RNA purification/extraction was performed.

Total RNA was isolated from livers collected from all groups using the RNeasy Micro Kit (QIAGEN, Hilden, Germany) according to the manufacturer's instructions. Total RNA levels in the final eluent were determined using a Nanodrop 2000C spectrophotometer (Thermo Fisher Scientific).

First-strand complementary DNA (cDNA) was synthesized using the RevertAid™ First Strand cDNA Synthesis Kit (K1622; Thermo Fisher Scientific). One thousand nanograms of total RNA were reverse transcribed in a total volume of 20 µL for 60 min at 42°C according to the manufacturer's instructions. The reaction was terminated by heating at 70°C for 5 min (**Table 4**).

5.3. RT-qPCR analyses

The cDNA levels were then analyzed using a QuantStudio™ 5 Real-Time PCR System (Thermo Fisher Scientific) using SYBR Green detection. Approximately 10 μg of total cDNA was used for the RT-PCR in a 20 μL reaction mixture comprising 0.1 μL stock solution (100 pmol) of suitable forward and reverse primers for the target genes, 10 μL of 2×GoTaq® qPCR Master Mix (Promega Corp., Madison, WI, USA), and 0.4 μL CXR (Promega A6001/2; Promega Corp.). Real-time PCR was performed with an initial denaturation of 2 min at 95°C, followed by 40 cycles of 15 s at 95°C, 30 s at 53°C, and 30s at 61°C.

The relative mRNA levels of the nuclear hormone receptors and CYP enzymes were calculated using the $2^{-\Delta\Delta CT}$ method [25]. The *glyceraldehyde 3-phosphate dehydrogenase* (*GAPDH*) gene was used as the housekeeping gene.

Table 3. Primers used for RT-qPCR.

Gene	Sequence of forward primer	Sequence of reverse primer	GenBank accession no.
Mouse *Cyp1a1*	5′- GGC CAC TTT GAC CCT TAC AA-3′	5′- CAG GTA ACG GAG GAC AGG AA-3′	NM_001136059.2
Mouse *Cyp2b10*	5′-TGA AGT ACT TTC CTG GTG CCC ACA-3′	5′-AGA AGG AGA AGT CCA ACC AGC ACA-3′	NM_009999.4
Mouse *Cyp3a11*	5′-CAG CTT GGT GCT CCT CTA CC-3′	5′-CTC TGG GTC TGT GAC AGC AA-3′	NM_007818.3
Mouse *Cyp4a10*	5′-TGA GGG AGA GCT GGA AAA GA-3′	5′-CTG TTG GTG ATC AGG GTG TG-3′	NM_010011.3
Mouse *GAPDH*	5′-AAC TTT GGC ATT GTG GAA GG-3′	5′-ACA CAT TGG GGG TAG GAA CA-3′	NM_001289726.1

Table 4. RT-qPCR thermal cycling conditions.

Step	Temperature (°C)	Time	Cycles
Initialization	95	2 min.	1x
Denaturation	95	15 sec.	
Annealing	53	30 sec.	40x
Extension	60	30 sec.	

6. Statistical analysis

All ordinary values are expressed as means ± standard deviations (SDs). Statistical significance was analyzed using SPSS (IBM SPSS Statistics Inc., Chicago, IL., USA). One-way ANOVA was used to compare three or more treatment groups followed by a post-hoc Tukey's test. $p \leq 0.05$ was regarded as significantly different from control values and shown in figures with an asterisk.

III. RESULTS

1. Body and organ weights

Body weights of the control group, the statin groups (LOW and HIGH), or the positive control drug groups (TCPOBOP, rifampicin, DEHP, and TCDD) were recorded immediately prior to dosing and on the day of sacrifice **(Figure 1)**. First, the average body weights of the statin groups were compared with those of the control group on days 1, 7, 14, 21, 28, 35, 49, and 56 (**Figure 1A, 1B**). Significant weight loss was observed in the female groups administered the statin-based drug (**Figure 1B**), but the maximal weight loss was only 14%. No significant differences were observed among the male groups (**Figure 1A**). There were no significant differences between the positive control groups and the control group (**Figure 1C, 1D**).

At necropsy, the absolute liver weights and thyroid glands were recorded, and the relative organ weights were calculated by dividing absolute weights by body weights **(Figure 2)**. The relative liver weight significantly increased compared with the CONTROL group for all treatment groups (**Figure 2A, 2C**). The relative liver weight of the LOW group increased by 4%–7%, and that of the HIGH group increased by 12%–15% (**Figure 2A**). The positive control groups' relative liver weights increased by a minimum of 17% and up to 2.6 times (**Figure 2C**). Overall, the liver weights of males increased more than those of the females. The relative thyroid glands weight significantly decreased in the TCPOBOP, Rifampicin, and DEHP group compared with

the control group (**Figure 2D**). There were no significant differences between the statin groups and the control group (**Figure 2B**).

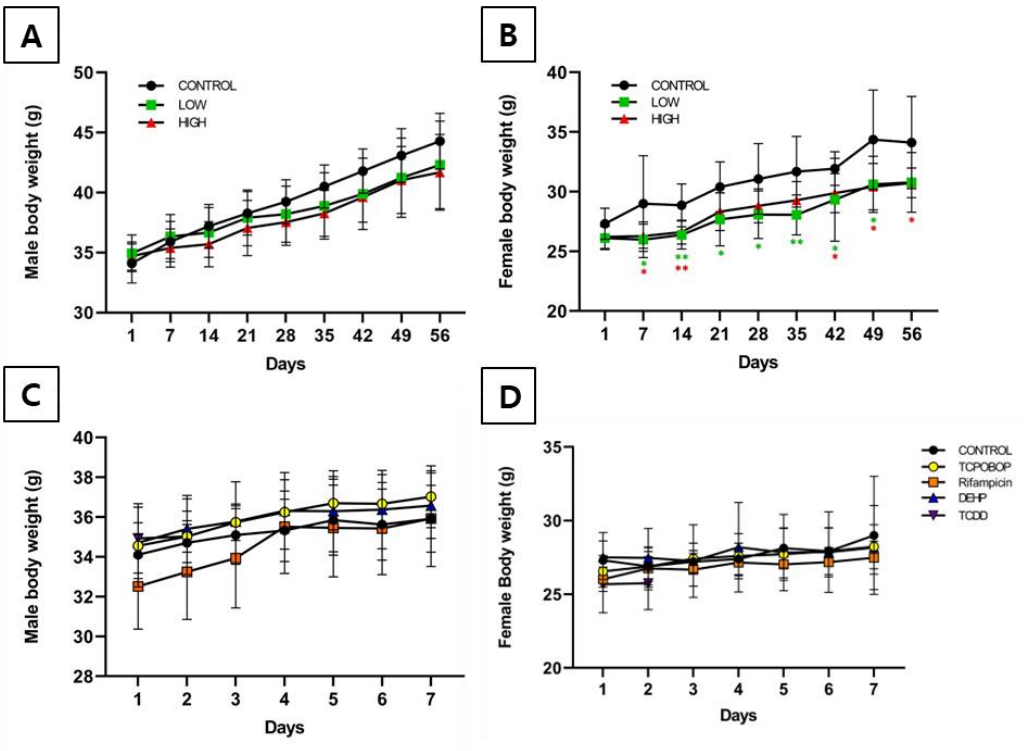

Figure 1. Changes in body weights during the drug administration period. The mean body weight gains in the female LOW and HIGH groups were lower than that of the CONTROL group during exposure (Figure 1B), but there were no significant weight losses in the other groups (Figure 1A, 1C, and 1D). Data are expressed as means ± standard deviations (SDs) of n=8 mice per group. *$p < 0.05$, **$p < 0.01$.

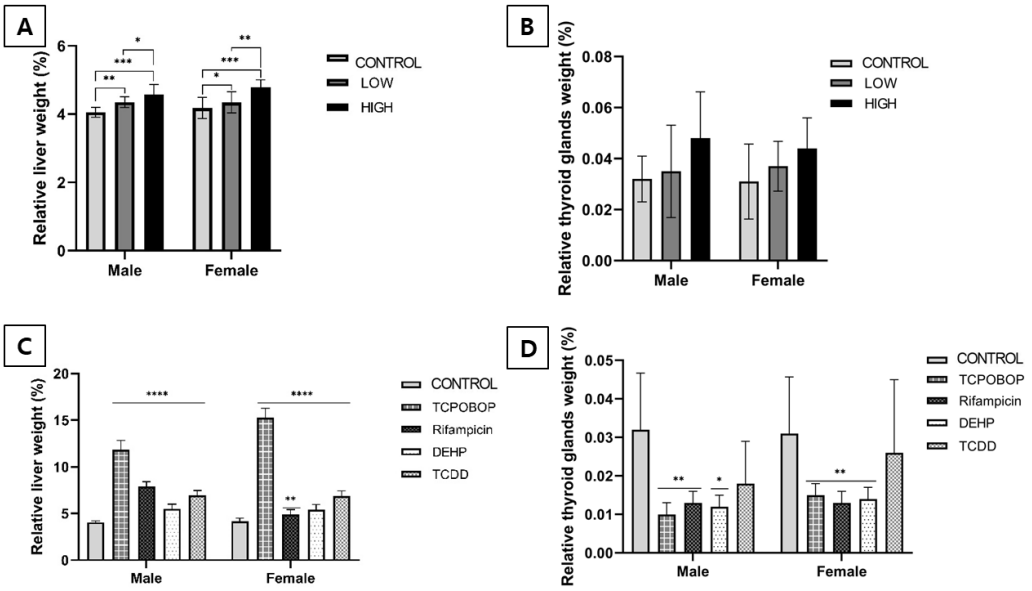

Figure 2. Relative organ weights of mice at the end of the drug administration period. Data are expressed as means ± standard deviations (SDs) of n=8 mice per group. *$p < 0.05$, **$p < 0.01$, ***$p < 0.001$, ****$p < 0.0001$.

2. Serum biochemistry

Alanine aminotransferase (ALT), aspartate aminotransferase (AST), alkaline phosphatase (ALP), total bilirubin (TBIL), triiodothyronine (T3), glucose, total protein (TP), and cholesterol levels were measured in the serum collected at necropsy.

In the statin groups, mean serum AST values increased 1.3-2 times and ALT values increased 1.4-3 times. In the TCPOBOP group, mean serum ALP levels increased 2.7-4.5 times, AST levels increased 2.3-3.9 times, and ALT levels increased 6.2-23 times. In the case of DEHP group, mean serum ALP values increased 1.6 times in the female group. In the TCDD group, mean serum ALP, AST, and ALT levels increased 1.4-1.6 times in the female group. There were no significant differences among the other values (**Table 5**).

Table 5. Results of serum biochemistry. Data are expressed as mean ± standard deviation (SD) of n=8 mice per group.

Group (Male)		GLU	CHO	TP	TBIL	ALP	AST	ALT	T3
Control	Mean	154.788	134.175	5.298	0.184	210.100	53.800	36.775	7.217
	SD	14.180	21.720	0.242	0.051	57.662	7.556	7.078	0.762
LOW	Mean	126.563	135.800	5.081	0.296	188.100	106.800	111.213	6.256
	SD	14.456	28.164	0.196	0.143	74.147	62.434	83.847	0.350
HIGH	Mean	132.075	116.800	5.255	0.194	212.763	103.850	84.963	5.840
	SD	39.753	27.002	0.220	0.053	27.339	43.048	51.446	1.360
TCPOBOP	Mean	158.871	73.600	5.129	0.012	953.057	126.543	227.414	5.474
	SD	41.724	28.994	0.342	0.018	675.905	52.367	113.078	0.650
Rifampicin	Mean	217.363	157.838	4.923	0.252	462.475	52.250	36.425	3.847
	SD	24.957	17.273	0.266	0.106	87.298	4.746	8.911	0.525
DEHP	Mean	196.400	148.438	4.985	0.115	282.325	52.075	27.975	3.746
	SD	35.602	23.541	0.108	0.040	82.075	5.917	8.143	0.599
TCDD	Mean	221.988	146.963	4.969	-0.003	243.550	54.800	37.250	4.402
	SD	68.915	13.428	0.570	0.048	57.432	17.316	14.689	0.789

Group (Female)		GLU	CHO	TP	TBIL	ALP	AST	ALT	T3
Control	Mean	134.163	94.425	5.214	0.071	242.938	71.988	43.025	6.501
	SD	19.395	19.630	0.154	0.018	53.348	29.302	35.798	0.302
LOW	Mean	118.138	76.025	5.111	0.066	266.738	91.900	62.588	6.291
	SD	24.719	14.428	0.178	0.017	60.587	18.160	21.625	0.921
HIGH	Mean	138.588	81.013	5.018	0.055	266.563	116.750	75.900	5.730
	SD	10.162	26.752	0.174	0.034	28.790	63.873	42.101	0.970
TCPOBOP	Mean	178.488	85.675	5.234	-0.002	650.900	282.275	990.300	3.411
	SD	43.702	28.340	0.613	0.017	378.287	142.678	617.450	1.302
Rifampicin	Mean	198.538	121.375	5.044	0.177	384.250	48.713	23.288	3.337
	SD	31.173	23.964	0.347	0.051	116.249	2.999	3.456	0.532
DEHP	Mean	211.438	117.663	5.023	0.050	382.488	88.775	28.513	3.681
	SD	52.342	21.926	0.236	0.059	149.381	118.415	6.540	0.573
TCDD	Mean	195.413	102.288	4.933	-0.028	341.725	104.363	67.488	3.848
	SD	45.269	20.917	0.361	0.040	55.195	62.721	80.467	0.730

3. Histopathological examination of mouse livers

Some histopathological findings of hepatocytes include centrilobular hepatocellular hypertrophy compared with the CONTROL group for all treatment groups. Parenchymal necrosis with inflammatory cell infiltration and micro-vacuolation was also observed occasionally **(Figure 3)**.

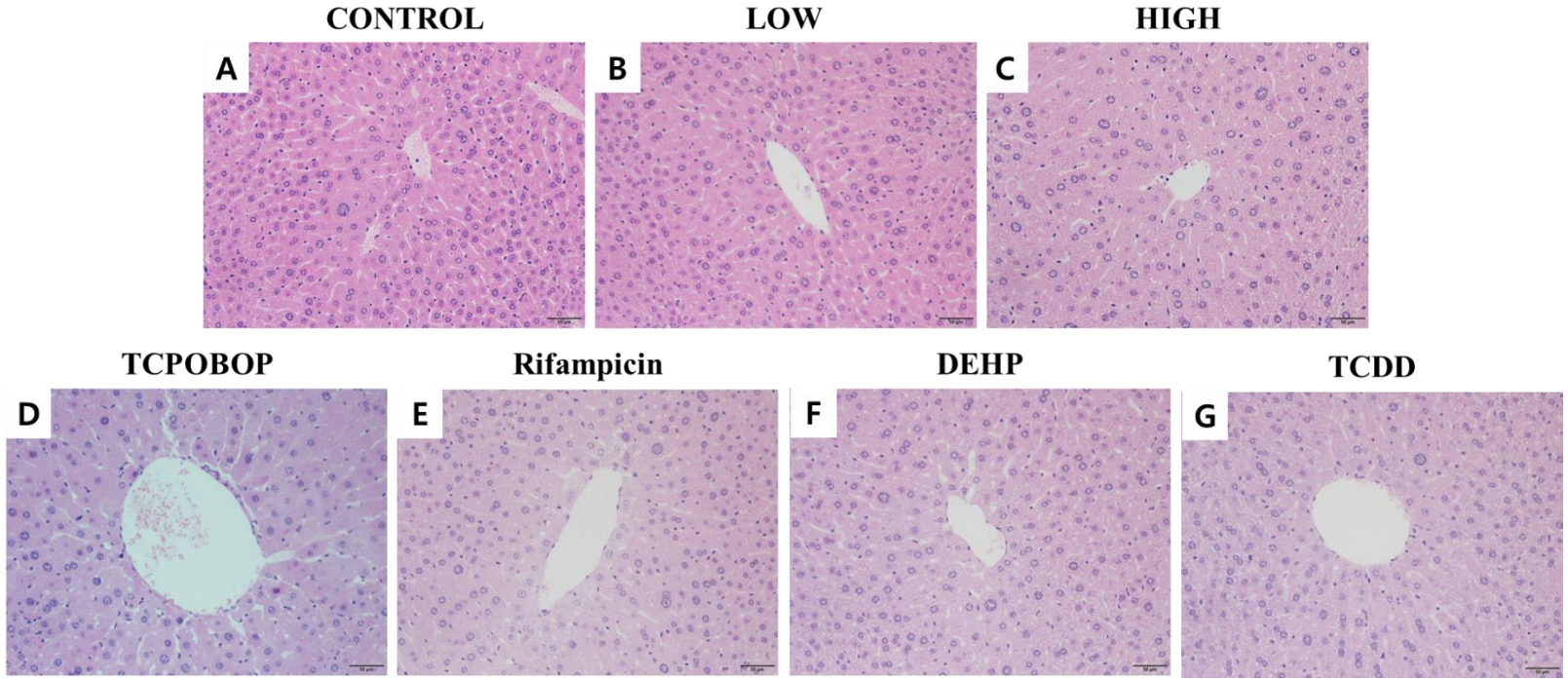

Figure 3. Histopathological examination of mice livers after statin-based drug administration. The representative microscopic images of liver paraffin sections. Histopathological findings include centrilobular hepatocellular hypertrophy (Figure 3C, D, E, F and G). H&E staining, 200× magnification, scale bar=50 μm.

4. Immunohistochemistry for CYP1A1, CYP2B10, CYP3A4, and CYP4A10

The positive immunostaining for CYP1A1 in the TCPOBOP and TCDD group were characterized by foci in the hepatocyte cytoplasmic staining (**Figure 4A4, 4A7**), while CYP1A1 staining of the other groups were not observed. CYP2B10 was extensively and prominently stained in the hepatocyte cytoplasm near the portal vein in the TCPOBOP-treated group (**Figure 4B4**). This pattern was similar to that of the statin groups, but no significant difference were observed compared with the CONTROL group (**Figure 4B1-3**). CYP3A4 was extensively stained in groups treated with TCPOBOP and Rifampicin (**Figure 4C4, 4C5**), and more strongly stained in the LOW group compared with CONTROL group (**Figure 4C1, 4C2**). The cytoplasms of hepatocytes were stained for CYP4A10, and the group treated with DEHP was stained much more strongly than the others (**Figure 4D6**). It was also stained in the statin groups, but no significant difference was observed compared with the CONTROL group (**Figure 4D1-3**).

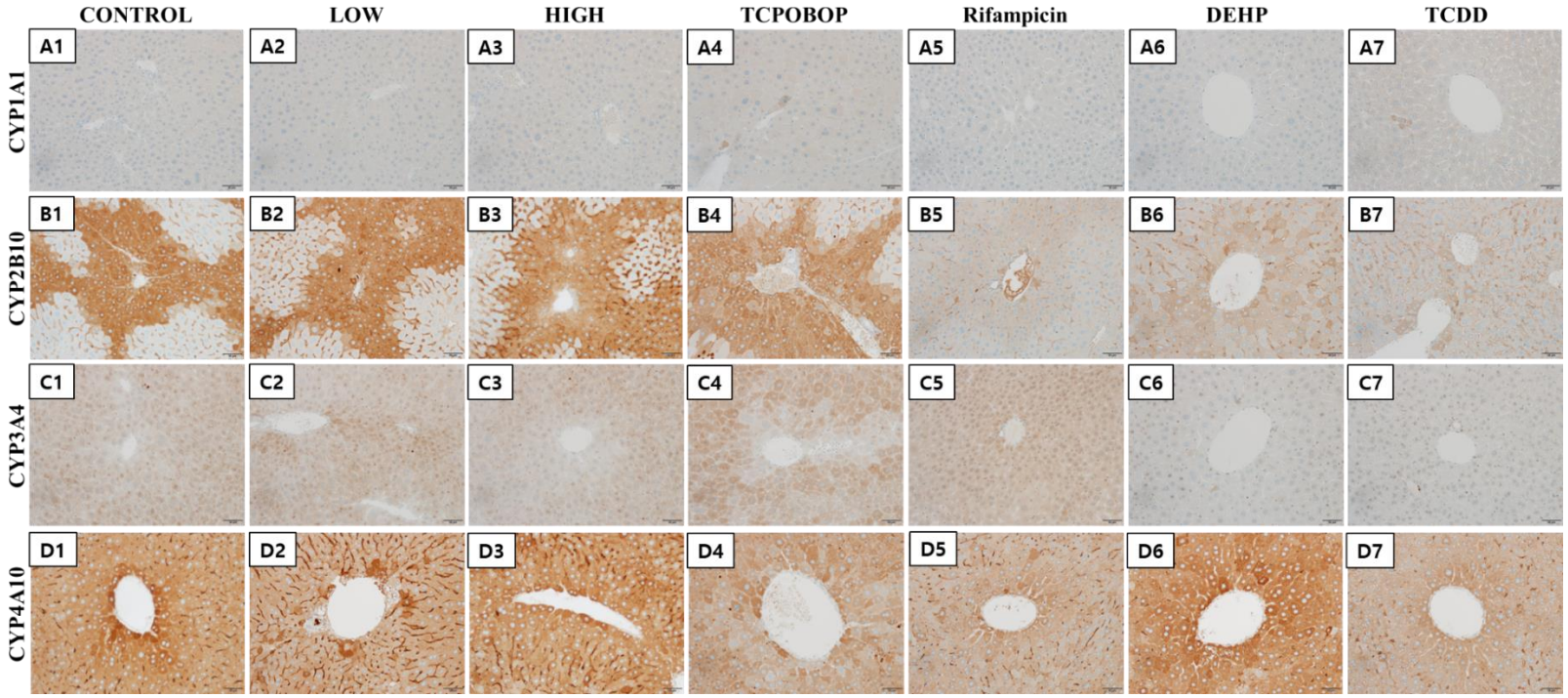

Figure 4. Immunohistochemical analyses of CYP1A1, CYP2B10, CYP3A4, and CYP4A10 in male mice livers. The representative images of the immunohistochemical results for CYP1A1 (Figure 4A1-7), CYP2B10 (Figure 4B1-7), CYP3A4 (Figure 4C1-7), and CYP4A10 (Figure 4D1-7). Formalin-fixed, paraffin-embedded sections, 400× magnification, scale bar=50 μm.

5. RT-qPCR for *Cyp1a1, Cyp2b10, Cyp3a11*, and *Cyp4a10*

The typical *Cyp* mRNA levels (*Cyp1a1, Cyp2b10, Cyp3a11*, and *Cyp4a10*) in mice were also analyzed to evaluate the effects of the statin-based test article mediated by AhR, CAR, PXR, and PPARα, respectively.

From *Cyp3a11* was highly expressed identified to have high expression levels more than 4-fold both in the LOW and HIGH groups, with a more than 4-fold increase over its expression compared with that in the CONTROL group in males (**Figure 7A**). For the positive control groups compared with the CONTROL group, the expression increases of *Cyp1a1*, *Cyp2b10*, and *Cyp3a11* expression levels increased to a similar extent in the positive control groups were observed in common (**Figure 5B, 6B, and 7B**). *Cyp1a1* levels increased the most in TCDD. *Cyp2b10* and *Cyp3a11* levels increased the most in TCPOBOP. For In *Cyp4a10*, statistically significant numerical reductions in expression were only observed in the only in the groups administered TCPOBOP or rifampicin (**Figure 8B**).

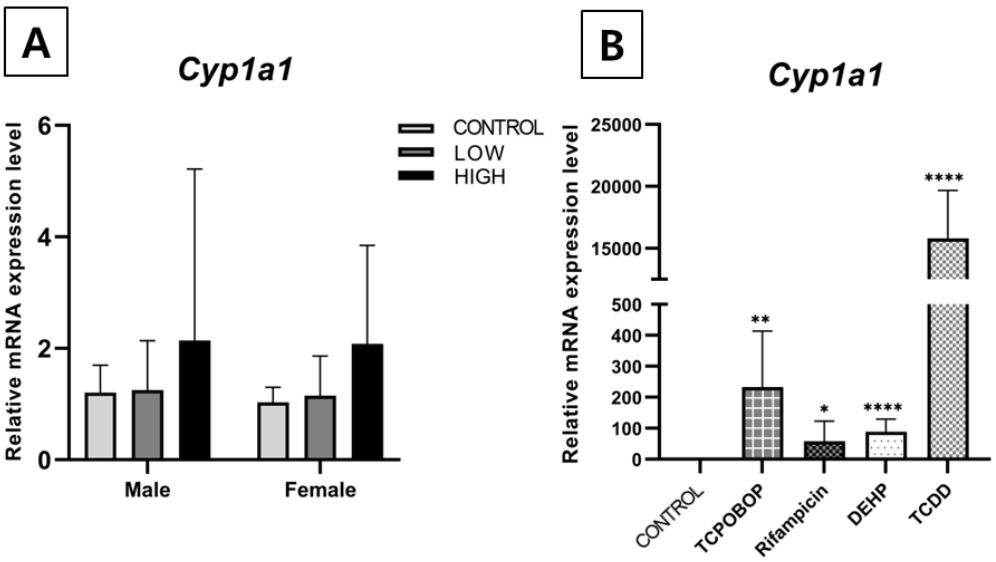

Figure 5. RT-qPCR for *Cyp1a1* in mouse livers. Data are expressed as means ± standard deviations (SDs) of n=8 mice per group. *$p < 0.05$, **$p < 0.01$, ****$p < 0.0001$.

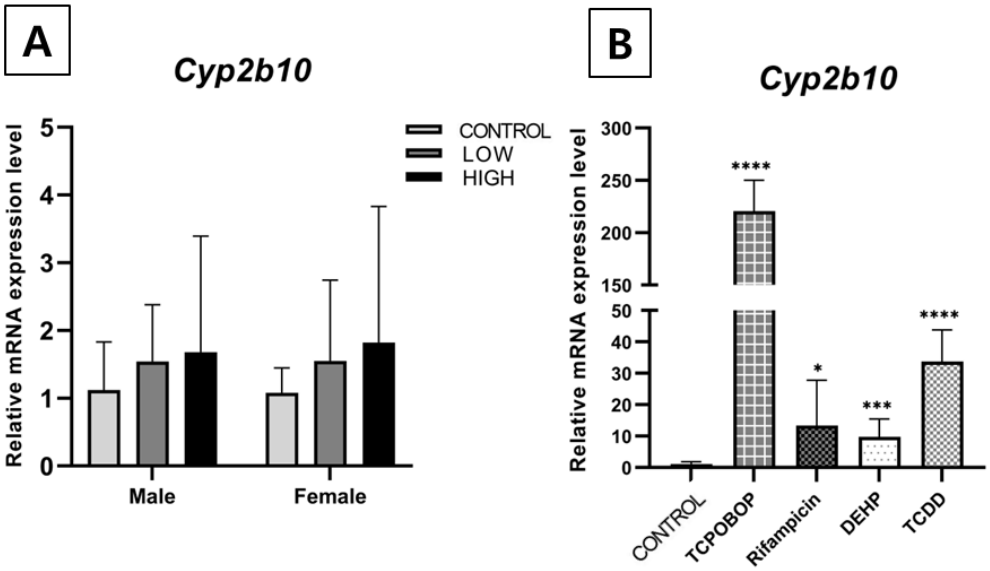

Figure 6. RT-qPCR for *Cyp2b10* in mouse livers. Data are expressed as means ± standard deviations (SDs) of n=8 mice per group. *$p < 0.05$, ***$p < 0.001$, ****$p < 0.0001$.

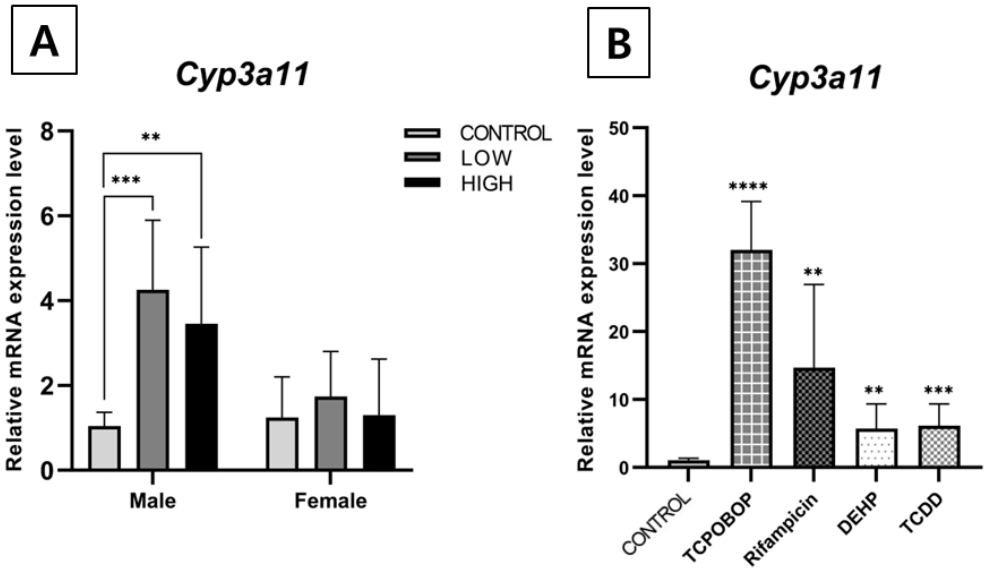

Figure 7. RT-qPCR for *Cyp3a11* in mouse livers. Data are expressed as mean ± standard deviations (SDs) of n=8 mice per group. *$p < 0.05$, **$p < 0.01$, ***$p < 0.001$, ****$p < 0.0001$.

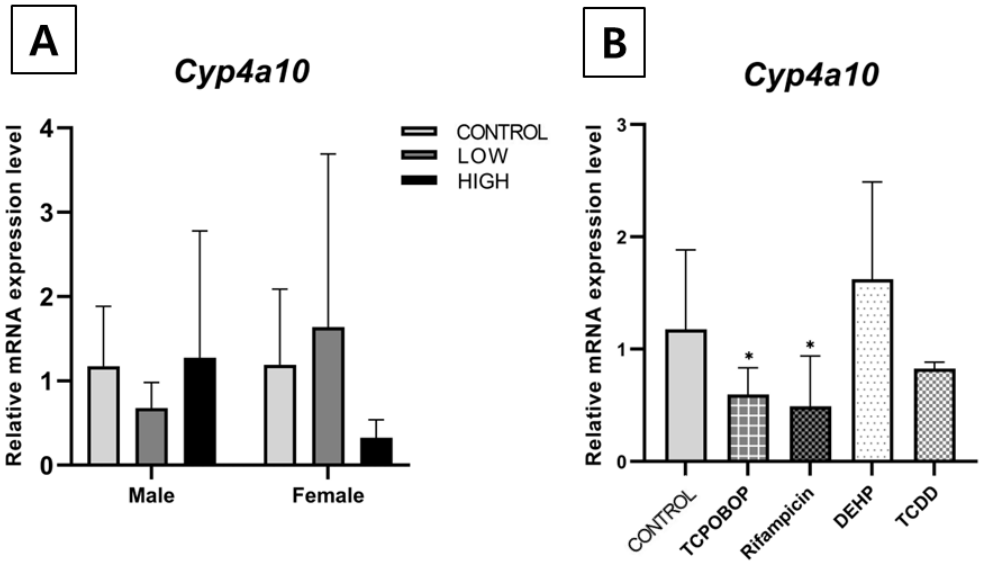

Figure 8. RT-qPCR for *Cyp4a10* in mouse livers. Data are expressed as means ± standard deviations (SDs) of n=8 mice per group. *$p < 0.05$.

IV. DISCUSSION

Liver enlargement in rodents is usually detected by the measurement of an increase in organ weight and the data can provide sensitive indices of toxicologic change where it can correlate and confirm changes observed through the microscope [21].

Relative liver weights increased by up to 15% in the HIGH group and increased by a minimum of 17% to a maximum of 2.6 times in the positive control groups. Alterations in liver weight may suggest treatment-related changes since the weight changes appeared to be dose-dependent. In the histopathological findings of the liver, centrilobular hepatocellular hypertrophy was observed. It appeared to be more frequent and severe in the HIGH group. Centrilobular hepatocellular hypertrophy is a histopathological feature of enzyme induction, which is thought to be correlated with changes in liver weight [26, 27].

The increased levels of AST and ALT in serum biochemistry assessment seems to be associated with parenchymal necrosis and inflammatory cell infiltration observed in histopathological examination. It seems to be caused by the mechanical effects of compression as the size of the liver increased.

Cyp3a11 mRNA levels in the LOW and HIGH groups were approximately 3-4 times higher than those of the CONTROL group, and in mice treated with rifampicin, which activates PXR, *Cyp3a11* expression was more than 15 times higher than in the CONTROL group. Significant differences in immunostaining intensity for CYP3A4 was stained more strongly than the CONTROL group, which had similar patterns in the

rifampicin group. The higher expressions of CYP3A levels in the LOW group than in the HIGH group were likely due to autoinduction in which the administered drug was decomposed due to enzyme induction by the test article at the high dose.

The therapeutic class of HMG-CoA reductase inhibitors, or statins, are central agents in the treatment of hypercholesterolemia and the associated conditions of cardiovascular disease, obesity, and metabolic syndrome [28]. Statins lower serum LDL-c (low-density lipoprotein cholesterol) concentrations to reduce cardiovascular morbidity and mortality [29]. All statins are relatively hepatoselective because most endogenous cholesterol production occurs in the liver [30]. As the predominant route of elimination for the majority of statins is through bile after metabolism by the liver [31], the liver is considered to be the target organ for statins. Statins are predominantly metabolized by CYP3A4, which belongs to the CYP family [30, 32]; CYPs have been identified as potential agonists for the PXR (pregnane X receptor), which they regulate [28]. Our study appears to support this finding. PXR activation might probably also be involved in the regulation of hepatocyte proliferation, but it is currently not considered a relevant factor in liver tumor promotion.

In conclusion, the statin-based drug-induced hepatic proliferative changes are likely to be mediated by CYP3A subfamily, suggesting that these changes are less relevant in humans.

RERERENCES

1. Plant, N., *Interaction networks: coordinating responses to xenobiotic exposure.* Toxicology, 2004. **202**(1-2): p. 21-32.
2. OINONEN, T. and O.K. LINDROS, *Zonation of hepatic cytochrome P-450 expression and regulation.* Biochemical Journal, 1998. **329**(1): p. 17-35.
3. Amacher, D., S. Schomaker, and J. Burkhardt, *The relationship among microsomal enzyme induction, liver weight and histological change in rat toxicology studies.* Food and chemical toxicology, 1998. **36**(9-10): p. 831-839.
4. Korzekwa, K., *Enzyme kinetics of oxidative metabolism: cytochromes P450.* Enzyme Kinetics in Drug Metabolism, 2014: p. 149-166.
5. Waxman, D.J., *P450 gene induction by structurally diverse xenochemicals: central role of nuclear receptors CAR, PXR, and PPAR.* Archives of biochemistry and biophysics, 1999. **369**(1): p. 11-23.
6. Marx-Stoelting, P., C. Knebel, and A. Braeuning, *The connection of azole fungicides with xeno-sensing nuclear receptors, drug metabolism and hepatotoxicity.* Cells, 2020. **9**(5): p. 1192.
7. Schwarz, M. and K.E. Appel, *Carcinogenic risks of dioxin: mechanistic considerations.* Regulatory Toxicology and Pharmacology, 2005. **43**(1): p. 19-34.
8. Bock, K.W. and C. Köhle, *Ah receptor-and TCDD-mediated liver tumor promotion: clonal selection and expansion of cells evading growth arrest and apoptosis.* Biochemical pharmacology, 2005. **69**(10): p. 1403-1408.
9. Kasai, T., et al., *Two-year inhalation study of carcinogenicity and chronic toxicity of 1, 4-dioxane in male rats.* Inhalation toxicology, 2009. **21**(11): p. 889-897.
10. Maronpot, R.R., et al., *Hepatic enzyme induction: histopathology.* Toxicologic pathology, 2010. **38**(5): p. 776-795.
11. Yoshizawa, K., et al., *A critical comparison of murine pathology and epidemiological data of TCDD, PCB126, and PeCDF.* Toxicologic pathology, 2007. **35**(7): p. 865-879.
12. Wei, P., et al., *The nuclear receptor CAR mediates specific xenobiotic induction of drug metabolism.* Nature, 2000. **407**(6806): p. 920-923.
13. POLAND, A., et al., *1, 4-Bis [2-(3, 5-dichloropyridyloxy)] benzene, a potent phenobarbital-like inducer of microsomal monooxygenase activity.* Molecular pharmacology, 1980. **18**(3): p. 571-580.
14. Massey, E. and W. Butler, *Zonal changes in the rat liver after chronic administration of phenobarbitone: an ultrastructural, morphometric and biochemical correlation.* Chemico-Biological Interactions, 1979. **24**(3): p. 329-344.
15. Moore, J.T. and S.A. Kliewer, *Use of the nuclear receptor PXR to predict drug interactions.* Toxicology, 2000. **153**(1-3): p. 1-10.
16. Chrencik, J.E., et al., *Structural disorder in the complex of human pregnane X receptor and the macrolide antibiotic rifampicin.* Molecular Endocrinology, 2005. **19**(5): p. 1125-1134.
17. Cariello, N.F., et al., *Gene expression profiling of the PPAR-alpha agonist ciprofibrate in the cynomolgus monkey liver.* Toxicological Sciences, 2005. **88**(1): p. 250-264.
18. Klaunig, J.E., et al., *PPARα agonist-induced rodent tumors: modes of action and human relevance.* Critical reviews in toxicology, 2003. **33**(6): p. 655-780.
19. Bentley, P., et al., *Hepatic peroxisome proliferation in rodents and its significance for humans.* Food and Chemical Toxicology, 1993. **31**(11): p. 857-907.
20. Stott, W., *Chemically induced proliferation of peroxisomes: implications for risk*

assessment. Regulatory toxicology and pharmacology, 1988. **8**(2): p. 125-159.
21. Hall, A., et al., *Liver hypertrophy: a review of adaptive (adverse and non-adverse) changes—conclusions from the 3rd International ESTP Expert Workshop.* Toxicologic pathology, 2012. **40**(7): p. 971-994.
22. Sahota, P.S., et al., *Toxicologic pathology: nonclinical safety assessment*. 2013: CRC press.
23. Committee, E.S., et al., *Guidance on the use of the weight of evidence approach in scientific assessments.* Efsa Journal, 2017. **15**(8): p. e04971.
24. Rozen, S. and H. Skaletsky, *Primer3 on the WWW for general users and for biologist programmers*, in *Bioinformatics methods and protocols*. 2000, Springer. p. 365-386.
25. Rao, X., et al., *An improvement of the 2ˆ (–delta delta CT) method for quantitative real-time polymerase chain reaction data analysis.* Biostatistics, bioinformatics and biomathematics, 2013. **3**(3): p. 71.
26. Sellers, R.S., et al., *Society of Toxicologic Pathology position paper: organ weight recommendations for toxicology studies.* Toxicologic pathology, 2007. **35**(5): p. 751-755.
27. Juberg, D.R., et al., *The effect of fenbuconazole on cell proliferation and enzyme induction in the liver of female CD1 mice.* Toxicology and applied pharmacology, 2006. **214**(2): p. 178-187.
28. Howe, K., et al., *The statin class of HMG-CoA reductase inhibitors demonstrate differential activation of the nuclear receptors PXR, CAR and FXR, as well as their downstream target genes.* Xenobiotica, 2011. **41**(7): p. 519-529.
29. Ward, N.C., G.F. Watts, and R.H. Eckel, *Statin toxicity: mechanistic insights and clinical implications.* Circulation Research, 2019. **124**(2): p. 328-350.
30. Schachter, M., *Chemical, pharmacokinetic and pharmacodynamic properties of statins: an update.* Fundamental & clinical pharmacology, 2005. **19**(1): p. 117-125.
31. Knopp, R.H., *Drug treatment of lipid disorders.* New England Journal of Medicine, 1999. **341**(7): p. 498-511.
32. Bottorff, M. and P. Hansten, *Long-term safety of hepatic hydroxymethyl glutaryl coenzyme A reductase inhibitors: the role of metabolism—monograph for physicians.* Archives of internal medicine, 2000. **160**(15): p. 2273-2280.

국문요약

스타틴 계열 시험물질에 의해서 유도된 설치류 간 증식성 병변의 사람연관성 연구

설치류에서 간 비대(hepatomegaly) 및 간 암(hepatoma)과 같은 간 증식성 변화는 독성 연구에서 흔히 나타날 수 있다. 간 비대는 발암성 연구와 같은 장기 연구에서 간암으로 이어질 수도 있으나, 간 독성을 나타내는 조직학적 혹은 임상병리학적 변화가 없는 간 비대는 일반적으로 적응성 변화로 간주된다. 그러나, 간 증식성 병변에 대한 사람연관성은 작용기전에 따라 다양하게 해석될 수 있으며, 설치류 시험에서 발암성이 관찰되었을지라도 발생 기전에 따라 사람 연관성이 없을 수도 있다.

간 비대(hepatomegaly)는 간의 사이토크롬 P450 에 의해 유도되는 효소유도(enzyme induction)에 의해 나타날 수 있다. 효소 유도는 시험물질에 대한 일련의 대사 반응으로, 간의 무게 증가, 간세포의 형태학적 변화 및 CYP 유전자 발현 유도로 나타난다. 간 효소 유도의 형태학적 특징은 간 무게의 증가를 특징으로 하는 적응성의 생리학적 반응에서, 독성 및 발암성을 포함한 유해한 반응에 이르기까지 다양하다. 형태학적인 특징은 광학현미경, 전자현미경 및 면역조직화학염색으로 평가할 수 있으며, 임상병리학적인 변화와 함께 해석되어야 한다.

대부분의 CYP 형태는 관련된 유전자 전사를 증가시키는 핵 수용체 매개

기전에 의해 유도된다. 대표적인 효소유도제들은 핵수용체 AhR, CAR, PXR, 그리고 PPARα 관련된 경로를 촉진하며, 이와 관련된 CYP 유전자로는 CYP1A, CYP2B, CYP3A, 그리고 CYP4A 로 알려져 있다.

이때, CAR, PXR 및 PPARα가 활성화되는 기전을 갖는 경우, 설치류 특이적 반응으로 간주되는 반면, AhR에 의해 매개되는 발암기전의 경우 사람연관성이 높은 것으로 알려져 있으므로 해석에 주의가 필요하다. 따라서 간 비대와 함께 관련 병리학적 소견이 관찰된다면 이것이 사람연관성이 있는지에 대한 여부를 이해하는 것이 중요하다.

본 연구는 ICR 마우스를 이용한 스타틴계 약물에 대한 24개월간의 발암성 연구에서 관찰된 간 신생물에 대한 기전을 이해하고, 이러한 병리학적 소견이 사람과 상관관계가 있는지 확인하기 위한 후속 연구이다.

본 시험에서 사용된 동물 종은 선행연구에서 사용된 것과 같은 종인 ICR 마우스를 이용하였고, 간 신생물이 관찰되었던 선행 연구를 모방하기 위해 시험물질을 최대 용량인 3200 mg/kg으로 56일간 매일 경구 투여하였으며, 저용량 투여군에는 500 mg/kg으로 투여하였다.

또한 핵 호르몬 수용체 AhR, CAR, PXR, 및 PPARα를 유도시키는 것으로 알려진 TCDD, TCPOBOP, Rifampicin 및 DEHP를 양성 대조군으로 설정하였으며, 각 핵 호르몬 수용체가 활성화되기에 적절한 것으로 생각되는 투여 기간 및 용량으로 1일 1회 경구 투여하였다. 양성대조군은 스타틴 투여 그룹과 CYP 발현 정도를 비교하기 위해 고려되었다. 이후 체중, 간 무게, 혈청 생화학적 검사 및 간의 조직병리학적 검사를 통해 간 비대 및 간의 효

소 유도가 잘 이루어졌는지 확인하고, 정량적 실시간 PCR 및 면역조직화학 염색 기법을 통해 핵수용체의 관련 유전자의 mRNA 수준 및 단백질 수준에서의 발현 정도를 확인하여 주로 어떤 CYP 유전자에 의해 변화가 유도되었는지 관찰하였다.

본 연구 결과, 스타틴 기반 약물의 간 증식성 변화는 CYP3A subfamily 의 유전자 발현과 상관성이 관찰되었으며, 이들은 나아가 PXR 와 연관된 대사 기전을 가질 것으로 여겨진다. PXR 은 간세포 증식의 조절에도 관여할 수 있지만, 현재 간 종양의 촉진과 관련된 인자로 간주되지는 않는다.

결론적으로, 스타틴 기반 약물에 나타난 간 증식성 변화는 사람연관성이 낮을 것으로 여겨지며, 이러한 결론은 설치류 시험에서 발암성이 관찰될지라도 사람연관성에 대한 결론은 증거가중치 접근 방식을 통해 도출되는 것이 중요하다는 점을 시사한다.

중심단어: Cytochrome P450 (CYP); Enzyme induction; Hepato-carcinogenesis; Hepatocellular hypertrophy; Hepatomegaly; Nuclear hormone receptor